Supplemental Figure legends

Figure S1. L1622I and R1788W variants cause tissue-specific AnkB deficiency without altering AnkB's secondary and tertiary structure *in vitro*. (A) Targeting constructs used for generating knock-in mice bearing the L1622I or R1788W AnkB variants by homologous recombination. (B) The CD spectrum of the wild-type 220-kDa AnkB protein is compared with the spectra of the L1622I and R1788W AnkB polypeptides. The spectrum of running buffer was used to estimate background levels. (C) Coomassie blue staining shows the kinetics of wild-type (WT), L1622I (LI), and R1788W (RW) AnkB proteins proteolytic digestion with α-chymotrypsin. Asterisk and bracket respectively indicate full-length 220-kDa AnkB and proteolytic fragments. Data shown in B, C is representative of two independent determinations.(D) Immunoblots of 220-kDa AnkB and GAPDH protein expression in indicated tissues (n=5 mice per group, six independent experiments).

Figure S2. L1622I and R1788W variants cause loss of a less stable AnkB subpopulation. (A) Immunoblots of 220-kDa AnkB and GAPDH protein expression in MEFs treated with cycloheximide for the indicated time points. (B) Quantification of AnkB/GAPDH expression ratio as a percentage of levels in untreated control MEF cells. (C). Levels of AnkB proteins in primary MEF cultures in the absence or after treatment with inhibitors of various protein clearance pathways. Protein expression is given as AnkB/GAPDH levels relative to the same ratio in untreated control MEF cells. Data represent mean ± SEM (n=3 independent experiments). *$p<0.05$, **$p<0.01$ and ***$p<0.001$, one-way ANOVA with Tukey post-test.

Figure S3. Oral glucose intolerance in young *AnkB*$^{R1788W/+}$ and *AnkB*$^{L1622I/+}$ mice. (A) Blood glucose levels in response to oral glucose (2 mg/kg body weight) corresponding to 3-month old *AnkB*$^{+/+}$, *AnkB*$^{R1788W/+}$, and *AnkB*$^{L1622I/+}$ mice. (B) Area under the curve (AUC) for oral glucose tolerance test (OGTT). (D) Total body weight at 3 months for mice of indicated genotypes. Data show mean ± SEM (n=10 mice per group) and is representative of three independent experiments. *p<0.05, **p<0.01 and ***p<0.001, one-way ANOVA with Tukey post-test.

Figure S4. Normal intraperitoneal glucose tolerance in young *AnkB*$^{L1622I/L1622I}$ and *AnkB*$^{R1788W/R1788W}$ mice. (A) Blood glucose levels in response to intraperitoneal glucose (2 mg/kg body weight) administration. (B) Area under the curve (AUC) for intraperitoneal glucose tolerance test (IPTT). Data show mean ± SEM (n=12 mice per group) and is representative of three independent experiments. *p<0.05, one-way ANOVA with Tukey post-test.

Figure S5. Young InsP3R haploinsufficient mice display normal insulin sensitivity. (A) Blood glucose levels in response to insulin administration (0.75U/kg) during an insulin tolerance test (ITT) for 3-month old control (*Itpr1*$^{+/+}$) and haploinsufficient InsP3R (*Itpr1*$^{+/-}$) mice. (B) Area under the curve (AUC) for an ITT. Data represent mean ± SEM. (n=10 mice per group). *p<0.05, **p<0.01 and ***p<0.001, two-tailed t-test.

Figure S6. AnkB variants cause age-dependent changes in hepatic insulin sensitivity. (A) Basal and insulin-stimulated (clamp) hepatic endogenous glucose production (EGP) rates determined during hyperinsulinemic euglycemic clamps for 3-month old (n=8) (A) and 10-month old (n=10) (C) mice. (B, D) Percentage of EGP suppression during clamp analysis for 3-month old (n=8) (B) and 10-month old (n=10) (D) mice. (E) Quantification of glucose-6-phosphatase (G6p), phosphoenolpyruvate carboxykinase 1 (Pepck1), and fructose 1, 6-bis phosphatase (Fbp1) transcript levels in liver of 3-month old mice. Levels of beta-actin transcript were used for normalization. Graph shown in E is representative of three independent determinations in three animals per each genotype. Data represent mean ± SEM. *$p<0.05$, **$p<0.01$ and ***$p<0.001$, one-way ANOVA with Tukey post-test).

Figure S7. Characterization of the interaction between ANK repeats of AnkB and the N-terminal portion of GLUT4. (A) Schematic diagram of the ANK repeat domain of AnkB and the amino acid sequence corresponding to either residues 1-24 of human GLUT4 or 1206-1233 of the known ankyrin-binding domain (ABD) of mouse L1CAM. (B) ITC titration of a peptide of hGLUT4 (1–24) to AnkB repeats (1-847) shows no direct interaction. (C) ITC titration of the ABD of mL1CAM (1206-1233) to AnkB repeats (1-847) is shown as a positive control.

Figure S8. MEF from *AnkB*$^{R1788W/R1788W}$ and *AnkB*$^{L1622I/L1622I}$ mice differentiate into more and bigger adipocytes. (A) Oil red O (top) and BODIPY 493/507 (bottom) staining of day 8 differentiated adipocytes. Images are representative of 5 independent experiments. Scale bar, 10

μm. (B-E). Quantification of (B) CCAAT/enhancer binding protein alpha (C/ebpα), (C) fatty acid binding protein 4/ adipocyte protein 2 (Fabp4/aP2), (D) perilipin (Plin), and (E) peroxisome proliferator-activated receptor gamma (Pparg) transcript levels in differentiated adipocytes at different days post-differentiation. Levels of the 18S ribosomal subunit transcript were used for normalization. Data represent mean ± SEM from 12 independent preparations. *p<0.05, **p<0.01 and ***p<0.001, one-way ANOVA with Tukey post-test.

Figure S9. Young *AnkB*$^{R1788W/R1788W}$ mice show normal expression of adipogenesis-promoting genes before the onset of adiposity. (A). Relative expression of adipogenesis transcription factors transcripts in adipose tissue of 3-month old congenic male *AnkB*$^{R1788W/R1788W}$ mice. (B-D) Relative expression of transcript levels for PPARg target genes in adipose tissue of *AnkB*$^{R1788W/R1788W}$ mice. Levels of the GAPDH transcript were used for normalization. All data is reported as relative quantity (RQ) of target mRNA/GAPDH mRNA in *AnkB*$^{R1788W/R1788W}$ adipocytes relative to the same ratio in *AnkB*$^{+/+}$ cells. Data represent the mean of three mice per genotype for one experiment. Multi-way ANOVA analysis were performed to select target genes that were differentially expressed. *p<0.05.

Figure S10. Reduced life-span and age-dependent changes in body weight and fasting glucose in *AnkB*$^{R1788W/+}$ and *AnkB*$^{L1622I/+}$ mice. (A) Fasting glucose levels. (B) Body weights at indicated time points. Data represent mean ± SEM (n=50 mice per group, *p<0.05, **p<0.01 and ***p<0.001, one-way ANOVA with Tukey post-test). (C) Percent of survival during a 34 month

long longevity study. (D) Reduced longevity of *AnkB*$^{R1788W/+}$ compared with *AnkB*$^{+/+}$ littermates and *AnkB*$^{L1622I/+}$ mice. Data for C and D were obtained from a total of n=100 mice per group, *p<0.05, **p<0.01, Mantel-Cox test.

Supplemental Methods

Mouse lines and animal care

AnkB knock-in mice bearing either the p.L1622I or p.R1788W human variants were generated by homologous recombination with help from the Duke Transgenic Mouse Facility. In details, the targeting constructs were created by screening a 129/SvJ mouse genomic BAC library (Incyte Genomics) with DNA probes specific for exon 19 (L1622I) or exon 22 (R1788W) of the *Ank2* gene. A 10kb genomic fragment containing the appropriate exon was subcloned into the pBS KS+ vector (Stratagene) to generate the knock-in allele by site-directed mutagenesis using the QuikChange Site-Directed Mutagenesis Kit (Agilent technologies). Knock-in plasmids were sequenced to confirm the presence of the CTG/ATC mutation for the p.L1622I conversion, or C/T for the p.R1788W conversion, and the correct DNA fragments subcloned into the pBS/STDRX vector, which contains a floxed neomycin resistance gene. The targeting DNA was linearized and electroporated into 129/SvJ blastocysts. Ankyrin B targeted knock-in embryonic stem cells that were both positive by PCR and Southern Blots screens were injected into C57Bl/6 blastocysts and transferred to the oviduct of pseudopregnant females and chimeric mice were bred with C57Bl/6 mice. Germline transmission of the respective mutation was confirmed both by DNA sequencing and RT-PCR of AnkB mRNA. The floxed neomycin gene was subsequently excised by crossing to CMV-Cre mice (Jackson Laboratory, stock # 006054). AnkB knock-in mice were bred to full congenicity in the C57Bl/6 background using the Speed Congenic service

from Jackson laboratories. Each congenic knock-in mouse line was kept in both heterozygous and homozygous states.

SNP genotyping was performed on mouse tail DNA using the ABI 7500 Taqman SNP genotyping system (Applied Biosystems), which uses a PCR-based allelic discrimination assay in a 96-well–plate format with a dual laser scanner. The sequence of the probes purchased from Applied Biosystems is as follows: L1622I:
5’-GCAGGAAGCTTCCAAAGAAAGCGAGTCTAGCGACCACCCGCCCATGGTCT
CCGAAGAAGACATATCTGTCGGTTATTCCACATTTCAGGATTGCCTCCCCA
AAACTGAAGGGGACAGCCCAGCAGCAGCA[CTG/ATC]TCTCCTCAAATGC
ACCAGGAGCCAGTTCAACAAGATTTCTCAGGGAAAACGCAAGACCAGCA
GGAATATTAGTGAGTTTCATAAGAAAGTCTGTTAAGTACAGTTCC-3’;
R1788W:
5’-CAAGGGCTCTGTACAGGGCTGACCTCAGTCTTCCTGTTCAAAGGCTATCA
CTAGTGTGGTTCCGTAACTCAAAAATAAGAGGGACTCATGAAATGTTTTT
CAGGTTACCCGGAAAATCATTAGG[C/T]GGTACGTTTCCTCTGATGGCACA
GAGAAGGAGGAGGTTACCATGCAGGGAATGCCTCAGGAGCCAGTCAACA
TTGAGGATGGGGACAATTATTCCAAAGTGATAAAGCGCGTGGT-3’.

Plasmids

Plasmid used in transfection experiments included: 3xHA-AnkB and AnkB-GFP previously generated in our laboratory (12). Myc-7x-GLUT4-GFP (gift from Dr. Jonathan S. Bogan) was modified using the QuikChange Site-Directed Mutagenesis Kit (Agilent technologies) and mutagenesis primer 5'-GCCACCATGCCGTCGGGTGCACAGCAGATCGGCTCTGAAG-3' to

generate the F5A Myc-GLUT4-GFP clone. The pcDNA3.2/v5-DEST hGlut4 plasmid (Addgene) was modified to include an exofacial anti-hemaglutinin (HA) epitope using mutagenesis primer 5'-GAG GCA GGG GCC TTA CCC CTA CGA CGT GCC TGA CTA CGC CGA GGG ACC CAG CTC-3'. The resulting HA-GLUT4 construct was further modified to mutate the FQQI sites at position 5-8 of the GLUT4 coding sequence to AAAA using the mutagenesis primer 5'-CTTCACCATGCCGTCGGGCGCCGCAGCAGCAGGCTCCGAAGATGGGGAACC 3'.

Antibodies

Affinity-purified rabbit antibodies against AnkB, InsP3R, and GFP were generated in our laboratory and have been previously described (70, 12). Other antibodies included rabbit anti-Glut4 (#ab654, abcam), mouse anti-alpha 1 sodium potassium ATPase (#ab7671, abcam), mouse anti-GAPDH (#MAB374, EMD Millipore), mouse anti-HA (#901501, BioLegend), chicken anti HA (#ET-HA100, Aves Labs) mouse anti-Myc (#sc-40, Santa Cruz Biotechnology), rabitt anti-glucagon (#180064, Zymed), and guinea pig anti-insulin (#180067, Invitrogen). Rabbit antibodies against GAPDH (#D16H11 XP), perilipin (#D1D8 XP), pan Akt (#C67E7) and pAkt (#Ser473, D9E XP) were all purchased from Cell Signaling Technologies. Secondary antibodies used for fluorescence imaging were purchased from Life Technologies and included donkey anti-rabbit IgG conjugated to Alexa Fluor 568 (#A10042), donkey anti-mouse IgG conjugated to Alexa Fluor 568 (#A10037), and goat anti-chicken conjugated to Alexa Fluor 647 (#A-21469). Fluorescent signals in western blot analysis were detected using goat anti-rabbit 800CW (#926-32211, LiCOR) and goat anti-mouse 680RD (#926-68070, LiCOR).

Tolerance tests and measurement of plasma metabolites

Metabolic analyses were performed in either 3-month old (n=10) or 10 month-old (n=12) male mice. Animals used for oral glucose tolerance test (OGTT) and insulin tolerance test (ITT) were fasted for 12 hours. For OGTT, 2 g/kg body weight of glucose (Sigma) was administered by oral gavage. For ITT mice were administered 0.75 U/kg body weight of recombinant human insulin (Humulin R, Elli Lily) by intraperitoneal injection. Blood samples were collected from the tail vein at 0, 30, 60, 90 and 120 min for both OGTT and ITT and analyzed with an Accucheck glucometer. For fasted or fed serum measurements, blood was collected from the submandibular vein before (0 min) or 30 min after oral or intraperitoneal glucose administration. Plasma insulin was measured using a mouse insulin-specific enzyme-linked immunosorbent assay (ELISA, Millipore). Levels of circulating fatty acid were measured by a spectrophotometric technique using the Wako NEFA Kit (Wako).

Histology

White adipose tissue and pancreas from neonatal, 3-month or 10-month mice were fixed in 4% paraformaldehyde (PFA) and paraffin-embedded, cut to 5-mm sections, and mounted on glass slides. Sections were rehydrated and permeabilized with xylene-ethanol and blocked with blocking buffer (1% bovine serum albumin (BSA), 1% fish oil gelatin, 5% horse serum, and 0.02% Tween 20 in phosphate-buffered saline (PBS) for 1 hour at room temperature. Tissue sections were then subsequently incubated overnight with primary antibodies at 4°C and with secondary antisera for 1.5 hours at 4°C, washed with PBS, and mounted in Vectashield mounting media (Vector Laboratories). To quantify adipocyte and pancreatic islet size, the diameters of

100 cells from five sections corresponding to five independent mice per each genotype in analysis were measured using the Volocity software (PerkinElmer).

Analysis of AnkB protein expression and turnover

Total protein homogenates from mouse brain, heart, WAT, liver, pancreatic islets and MEF were prepared in PBS containing 150 mM NaCl, 0.32M sucrose, 2 mM EDTA, 0.1% Triton X-100, 0.1% sodium deoxycholate, 0.1% SDS and protease inhibitors (10 μg/ml AEBSF, 30 μg/ml benzamidine, 10 μg/ml pepstatin, and 10 μg/ml leupeptin) (EMD Biosciences). Samples were diluted 1:1 v/v in 5x PAGE and resolved by SDS-PAGE and Western blot. Protein-antibody complexes were detected using I^{125}-labeled protein A/G (Pierce).

For analysis of AnkB turnover MEF grown in triplicate in 6 well plates were treated overnight with either 40 μM calpain inhibitor or 25 nM of the proteasomal inhibitor epoxomicin, or the lysosomal inhibitors leupeptin (10 μM) and NH4Cl (10 mM), or for 6 hours with 100 nM of the autophagy inhibitor wortmanin. In parallel experiments MEF were incubated with 1uM cycloheximide (Cx, Sigma) to inhibit protein synthesis. After 30 min, cells were washed with 1X PBS and fresh media was added. Cell lysates were prepared for each well in triplicate before before and after treatment. SDS-PAGE samples were prepared, resolved, and detected as described in the above paragraph. Protein levels were quantified by densitometry using the ImageQuant 5.2 software (Molecular Dynamics).

Quantitative PCR

RNA from brain, heart, white adipose tissue, liver, pancreatic islets, and mouse embryonic fibroblasts was isolated using the RNeasy kit or the RNeasy Lipid Tissue Kit (Qiagen) and

DNase treatment (Qiagen) according to the manufacturer's instructions and then used for cDNA synthesis using the SuperScript® III First-Strand Synthesis System (Invitrogen). Quantitative PCR was performed with the Applied Biosytems 7500 Fast RT-PCR system and SYBR Green detection reagent.

Quantification of full-length 220-kDa AnkB transcript levels was conducted using commercially available mouse gene specific assays from IDT DNA (Mm.PT.58.32861750). As an internal control for potential variability, gene transcript levels were normalized to GAPDH transcript level measured using a gene specific assay (Mm.PT.39a.1, IDT DNA). Primer sequences for transcripts of proteins involved in adipogenesis were designed with Primer Express Software (Applied Biosytems) Primers were as follows: Pparγ For 5'-GCATGGTGCCTTCGCTGA- 3' and Rev 5'-TGGCATCTCTGTGTCAACCATG-3'; C/ebpα For 5'-CAAGAACAGCAACGAGTACCG-3' and Rev 5'-GTCACTGGTCAACTCCAGCAC-3'; Fabp4 For 5'-GCACGGTCTCTCTGCAATC-3' and Rev 5'-ACAATCAATCAGCGCAGGA-3'; Plin For 5'-CTCCGGCCTTTCCTCTCTA-3' and Rev 5'-GGGGGAGTGATGACATGG-3', 18S For 5'-TAGCCTTTGCCATCACTGCC-3' and Rev 5'-CATGAGCATATCTTCGGCCC-3'. Analyses of liver gluconeogenesis transcripts was conducted using commercially available mouse gene specific assays from IDT DNA (G6p, Mm.PT.53a.11964858; Pepck1, Mm.PT.53a.11992693; Fbp1, Mm.PT.53a.5253147; Actb, Mm.PT.39a.22214843.g).

Isolation of plasma membrane fractions

3-month old *AnkB*$^{+/+}$, *AnkB*$^{R1788W/R1788W}$ and *AnkB*$^{L1622I/L1622I}$ male mice were fasted overnight, divided in two groups of 5 mice each per genotype, and injected subcutaneously with either 0.5 U/kg of insulin or with saline solution as a vehicle control. 30 minutes post injection mice were euthanized, and the hindlimb muscles and epididymal fat pads were carefully dissected out and snap-frozen in liquid nitrogen. Homogenization of skeletal muscle samples and isolation of plasma membrane fractions by subcellular fractionation on a discontinuous sucrose gradient was conducted at 4°C in a buffer containing 5mM NaN_3, 0.25M sucrose, 0.1mM phenylmethylsulfonylfluoride (PMSF), and 10mM $NaHCO_3$ at pH 7.0 as described (67). Likewise, adipocyte tissue was homogenized at 4°C in a buffer containing 20mM Tris pH 7.4, 1mM EDTA, and 0.25M sucrose and the plasma membrane fractions were obtained by differential ultracentrifugation as described (68). We also used a similar protocol for isolation of plasma membrane fractions from differentiated adipocytes. In this case cells were starved for 2 hours at 37°C in DMEM supplemented with 0.2% BSA, after which they either left untreated or stimulated for 5 or 15 minutes with 100 nM insulin (Humulin R, Elli Lily). For all described membrane isolation procedures, 100 µl of total protein homogenates were saved previous to the subcellular fractionation step and used in further analysis of the activation of the insulin signaling pathway (see below). The final pellets containing the membrane fractions were dissolved in 5xPAGE, and equal amounts of protein for each condition and genotype were solved by SDS-PAGE and Western Blot using both I^{125}-labeled protein A/G and fluorescently-labeled secondary antibody (LiCOR) detection methods. The association of the Glut4 transporter with plasma membranes was determined by quantification of the immunoblot signal using the ImageQuant 5.2 software (Molecular Dynamics), and expressed as relative to GAPDH signal.

Pancreatic islet isolation and insulin secretion assays

Pancreatic islets were isolated from 3-month old *AnkB*$^{+/+}$, *AnkB*$^{R1788W/R1788W}$ and *AnkB*$^{L1622I/L1622I}$ male mice by pancreatic perfusion and digestion with Liberase TL (Roche) as previously described (71). Islets were pre-incubated in Hanks' balanced salt solution (HBSS) supplemented with 0.5% BSA for 2 hours and transferred to fresh solution containing 2.8 mM glucose for 1 hour to assess basal insulin secretion. Islets were then incubated with the stimulating solution containing 16.8 mM glucose for 1 hour. Insulin concentrations were determined using the Mouse Insulin ELISA (Millipore) and normalized for insulin content.

Mouse embryonic fibroblast cultures and differentiation into adipocytes

Primary mouse embryonic fibroblast (MEF) cultures were established from postnatal day 0 (PND0) *AnkB*$^{+/+}$, *AnkB*$^{+/-}$, *AnkB*$^{R1788W/R1788W}$ and *AnkB*$^{L1622I/L1622I}$ mice following a described protocol (72). In brief, after removal of all internal organs bodies were minced and digested in Hibernate A (BrainBits) containing 1% tripsin (Invitrogen) and 1 mg/ml DNAse (Sigma) for 30 min at 37°C. Tissue was washed three times with Hibernate E, dissociated in MEF media (Dulbecco's modified Eagle's medium (DMEM, Invitrogen) supplemented with 10% fetal bovine serum (FBS, Invitrogen), non-essential amino-acids (MEM, Invitrogen), 2 mM glutamine (Invitrogen), and penicillin/streptomycin (Invitrogen)), and vigorously agitated for 30 seconds. Dissociated cells were then passed through a 100 μm cell strainer (VWR) to remove any residual non-dissociated tissue, pelleted by centrifugation at 1,000 rpm for 5 minutes, plated on a 100-mm tissue culture dishes containing MEF media and incubated at 37°C and 5% of CO2 until the culture reached 80% confluence. For imaging, MEF were plated onto collagen-coated dishes (MatTek).

48 hours post-confluence MEFs were induced to undergo adipogenic differentiation by incubation for two days in induction media (MEF media supplemented with 5 µg/mL insulin (Invitrogen), 1 µM dexamethasone (Sigma), and 0.5 mM 3-isobutyl-1-methylxanthine (IBMX, Sigma)). Induction media was replaced with MEF media two days after the start of differentiation and refreshed every 3 days until use.

Electroporation of differentiated adipocytes

Adipocytes differentiated from MEF were electroporated four days after induction of differentiation using a square wave BTX ECM 830 pulse generator (BTX-Harvard Apparatus) following the manufacturer protocol. In brief, either 15 µg of Myc-GLUT4-GFP or F5A Myc-GLUT4-GFP plasmids, alone or in combination with 20 µg of 3xHA-AnkB (for rescue experiments) in BTXpressTM solution (BTX-Harvard Apparatus) were electroporated into differentiated adipocytes by applying a 20 ms pulse (75V, 1Hz). Adipocytes were processed for immunofluorescence or other analysis between 24 to 48 hours following electroporation.

Analysis of GLUT4 translocation and endocytosis by immunofluorescence

Four days after induction of differentiation, adipocytes were electroporated with Myc-GLUT4-GFP plasmid alone or in combination with 3xHA-AnkB as described above. Cells were plated in collagen-coated glass bottom dishes (MatTek) containing MEF media and allowed to express the transgene for 48 hours. For the evaluation of GLUT4 translocation and endocytosis differentiated adipocytes were starved in serum free DMEM containing 0.2% BSA for 2 hours at

37°C. Cells were either treated or not (basal) with 100 nM insulin for 30 min at 37°C. The population of plasma membrane associated GLUT4 was labeled with mouse anti-Myc antibody for 1h on ice. Cells were quickly washed with ice-cold PBS, followed by 37°C PBS and warm MEF media, and either fixed with 4% PFA (basal and time 0) or incubated at 37°C for 5, 10, 15, 20, and 30 minutes to allow for GLUT4 internalization. At the indicated time points cells were fixed in 4% PFA for 15 min at RT, washed with PBS, permebealized with 0.05% Triton-X100, incubated with secondary antibodies for 1 hour at RT, washed with PBS and mounted in Vectashield. Fluorescent antibody labeling was visualized using a 780 laser scanning confocal microscope (Zeiss). Z stacks with optical sections of 0.3 μm intervals were collected using a 40x (1.3NA) oil objective lens using the zoom feature. Z-stack projections were analyzed using ImageJ (http://rsb.info.nih.gov/ij). In brief, the wand tool of ImageJ was used to trace the outer and inner sides of the membrane and to measure total fluorescent signal (A) and cytosol-associated fluorescent signal (B). The ratio of plasma membrane/cytosol Myc-GLUT4 signal was calculated as (A-B)/B.

Expression and purification of AnkB proteins and *in vitro* biochemical analysis

Histidine-tagged wild-type, L1622I, and R1788W 220-kDa AnkB proteins were expressed using a BacPak expression system (Clontech) and purified by NiNTA (GE Healthcare) affinity chromatography as previously reported (73). For circular dichroism spectroscopy each purified AnkB protein (0.5 μM) was dialyzed in buffer containing 5 mM K_3PO_4, pH 7.4, and 50 mM KaF and loaded onto a 1-mm path-length quartz cuvette. CD measurements were taken on an Aviv 62 DS model CD spectrometer (Aviv Biomedical) at 37 °C between wavelengths of 260 and 190 nm. The susceptibility to proteolytic digestion was assessed by coomassie blue staining of SDS-

PAGE gel after incubation of each purified AnkB protein in PBS containing 0.5 mM EDTA, 0.2 mM TCEP, and 1mM NaN_3 with 10 ng/ml α-chymotrypsin for 1 hour at 37°C.

Immunoprecipitation

Total protein homogenates from mouse skeletal muscle tissue were prepared in PBS containing 150 mM NaCl, 0.32M sucrose, 2 mM EDTA, 0.1% Triton X-100, 0.1% sodium deoxycholate, 0.1% SDS and protease inhibitors (10 μg/ml AEBSF, 30 μg/ml benzamidine, 10 μg/ml pepstatin, and 10 μg/ml leupeptin) (EMD Biosciences). Samples were centrifuged at 100,000 x g for 30 min and the supernatants were pre-cleared with Protein-G Dynabeads (Invitrogen) and subjected to immunoprecipitation using antibodies against AnkB, GLUT4, or control IgG. Immunoprecipitation samples were resolved by SDS-PAGE and Western blot and antibodies were detected as described above.

For co-immunoprecipitation experiments 6×10^6 HEK 293T cells (HEK 293T/17, ATCC CRL-11268) obtained from the American Tissue Culture collection were plated in 10-cm dishes and transfected with 4 μg of each plasmid using Lipofectamine 2000 (Invitrogen) according to the manufacturer's instructions. Cells were harvested 48 h after transfection and lysed in 0.5% Triton X-100 in lysis buffer (10 mM sodium phosphate, 0.32M sucrose, 2 mM EDTA, and protease inhibitors). Cell lysates were centrifuged at 100,000 x g for 30 min and the soluble fraction was collected and precleared by incubation with Protein-G Dynabeads. Co-immunoprecipitation experiments were performed using Protein-G Dynabeads (Invitrogen) and mouse anti-HA or rabbit anti-GFP antibodies. Immunoprecipitation samples were resolved by SDS-PAGE and Western blot as described above.

Isothermal Titration Calorimetry assay

Isotermal titration calorimetry (ITC) measurements were carried out on a VP-ITC Microcal calorimeter (Microcal) at 25℃ as described before (41). All proteins were in 50 mM Tris buffer containing 100 mM NaCl, 1 mM EDTA and 1 mM DTT at pH 7.5. High concentration (200 μM) of each binding partners assayed in this study, including the N-terminal portion (amino acids 1-24) of human GLUT4 and the known ankyrin-binding domain (amino acids 1206-1233) of mouse L1-cell adhesion molecule (L1CAM) (40) were loaded into the syringe, with the corresponding ankyrin repeats (ammino acids 1-847) of human ankyrin-B (20 μM) in the cell. Each titration point was performed by injecting a 10 μL aliquot of syringe protein into ankyrin protein samples in the cell at a time interval of 120 seconds to ensure that the titration peak returned to the baseline. The titration data were analyzed using the program Origin7.0 and fitted to a one-site binding model.

Oil Red O staining and quantification

MEFs at days 0, 2, 6, 10, and 14 after induction of differentiation were fixed with 4% paraformaldehyde in phosphate buffer saline (PFA-PBS), for 15 minutes at room temperature and stained with Oil Red O (Sigma) solution for 15 minutes. Cells were washed two times with PBS and lipid levels were quantified by reading optical density at 520 nm following extraction of Oil Red O from stained cells using isopropanol.

BODIPY staining of lipid droplets

Cultured adipocytes were stained with BODIPY 493/503 (Invitrogen) following the manufacturer's recommended protocol. In details, cells were washed with PBS, fixed with 4% PFA-PBS for 20 min at room temperature, stained for 15 min in the dark with a 10 μg/ml BODIPY 493/503 solution, washed five times with PBS, and mounted in Vectashield mounting media (Vector Laboratories).

Prediction of functional impact of nonsynonymous AnkB variants

SIFT (http://sift.jcvi.org/) (74) and PolyPhen-2 (75) (http://genetics.bwh.harvard.edu/pph2/) tools were used to predict the possible impact of human AnkB variants on the structure or function of AnkB.

Suplemental References

70. Mohler PJ, Gramolini AO, Bennett V. The ankyrin-B C-terminal domain determines activity of ankyrin-B/G chimeras in rescue of abnormal inositol 1,4,5-trisphosphate and ryanodine receptor distribution in ankyrin-B (-/-) neonatal cardiomyocytes. *J Biol Chem.* 2002; 277(12):10599–10607.

71. Hohmeier HE, Mulder H, Chen G, Henkel-Rieger R, Prentki M, Newgard CB. Isolation of INS-1–derived cell lines with robust ATP-sensitive K+ channel-dependent and -independent glucose-stimulated insulin secretion. *Diabetes*. 2000; 49(3):424–430.

72. Baerga R, Zhang Y, Chen PH, Goldman S, Jin S. Targeted deletion of autophagy-related 5 (atg5) impairs adipogenesis in a cellular model and in mice. *Autophagy*. 2009; 5(8):1118–1130.

73. Abdi KM, Mohler PJ, Davis JQ, Bennett V. Isoform specificity of ankyrin-B: a site in the divergent C-terminal domain is required for intramolecular association. *J Biol Chem*. 2006; 281(9):5741–5749.

74. Kumar PM, Henikoff S, Ng PC. Predicting the effects of coding non-synonymous variants on protein function using the SIFT algorithm. *Nat Protoc*. 2009; 4(7):1073–1081.

75. Adzhubei IA, Schmidt S, Peshkin L, Ramensky VE, Gerasimova A, Bork P, Kondrashov AS, Sunyaev SR. A method and server for predicting damaging missense mutations. *Nat Methods*. 2010; 7(4):248–249.

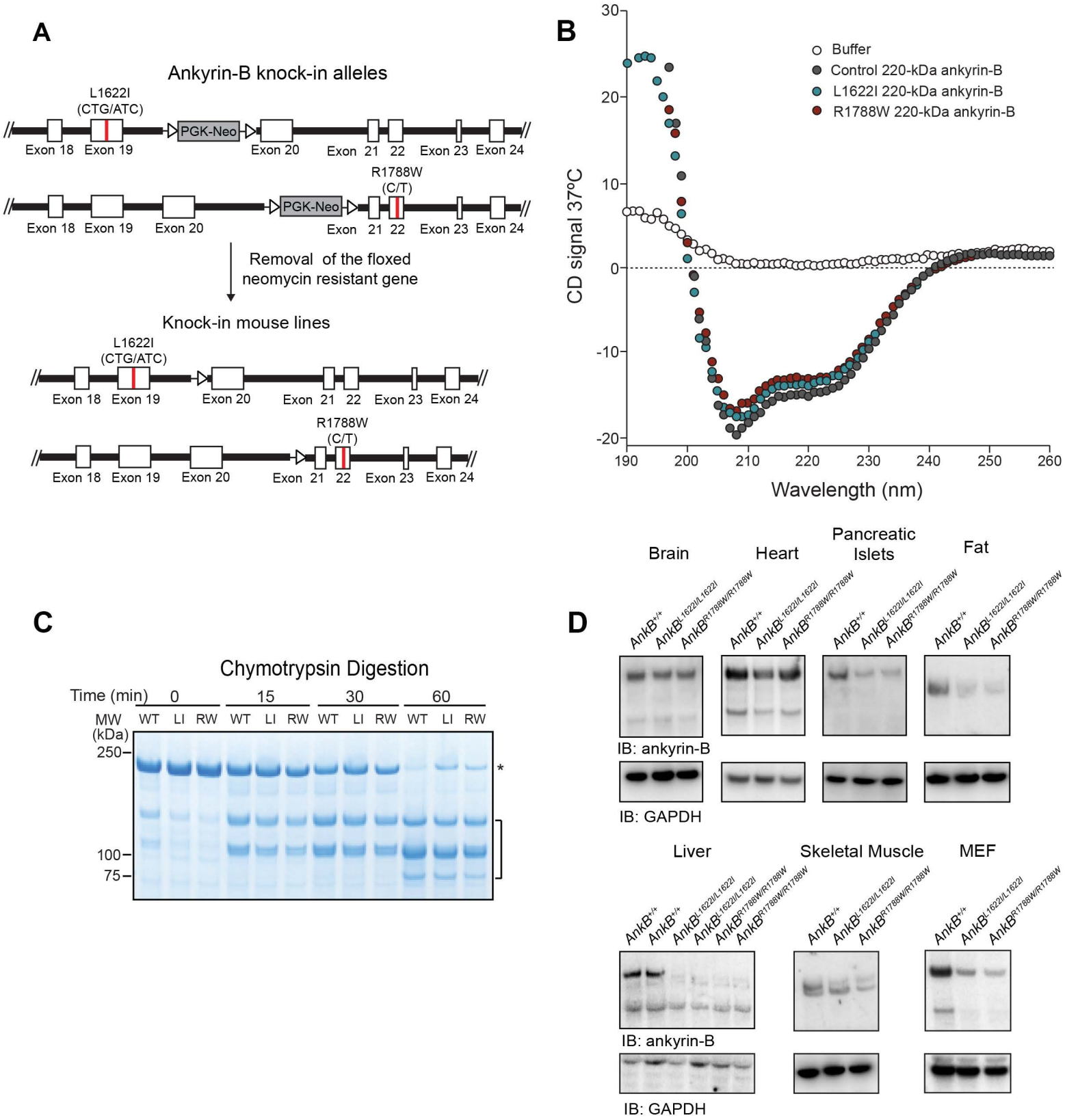

Figure S1. L1622I and R1788W variants cause tissue-specific AnkB deficiency without altering AnkB's secondary and tertiary structure *in vitro*. (A) Targeting constructs used for generating knock-in mice bearing the L1622I or R1788W AnkB variants by homologous recombination. (B) The CD spectrum of the wild-type 220-kDa AnkB protein is compared with the spectra of the L1622I and R1788W AnkB polypeptides. The spectrum of running buffer was used to estimate background levels. (C) Coomassie blue staining shows the kinetics of wild-type (WT), L1622I (LI), and R1788W (RW) AnkB proteins proteolytic digestion with α-chymotrypsin. Asterisk and bracket respectively indicate full-length 220-kDa AnkB and proteolytic fragments. Data shown in B, C is representative of two independent determinations.(D) Immunoblots of 220-kDa AnkB and GAPDH protein expression in indicated tissues (n=5 mice per group, six independent experiments).

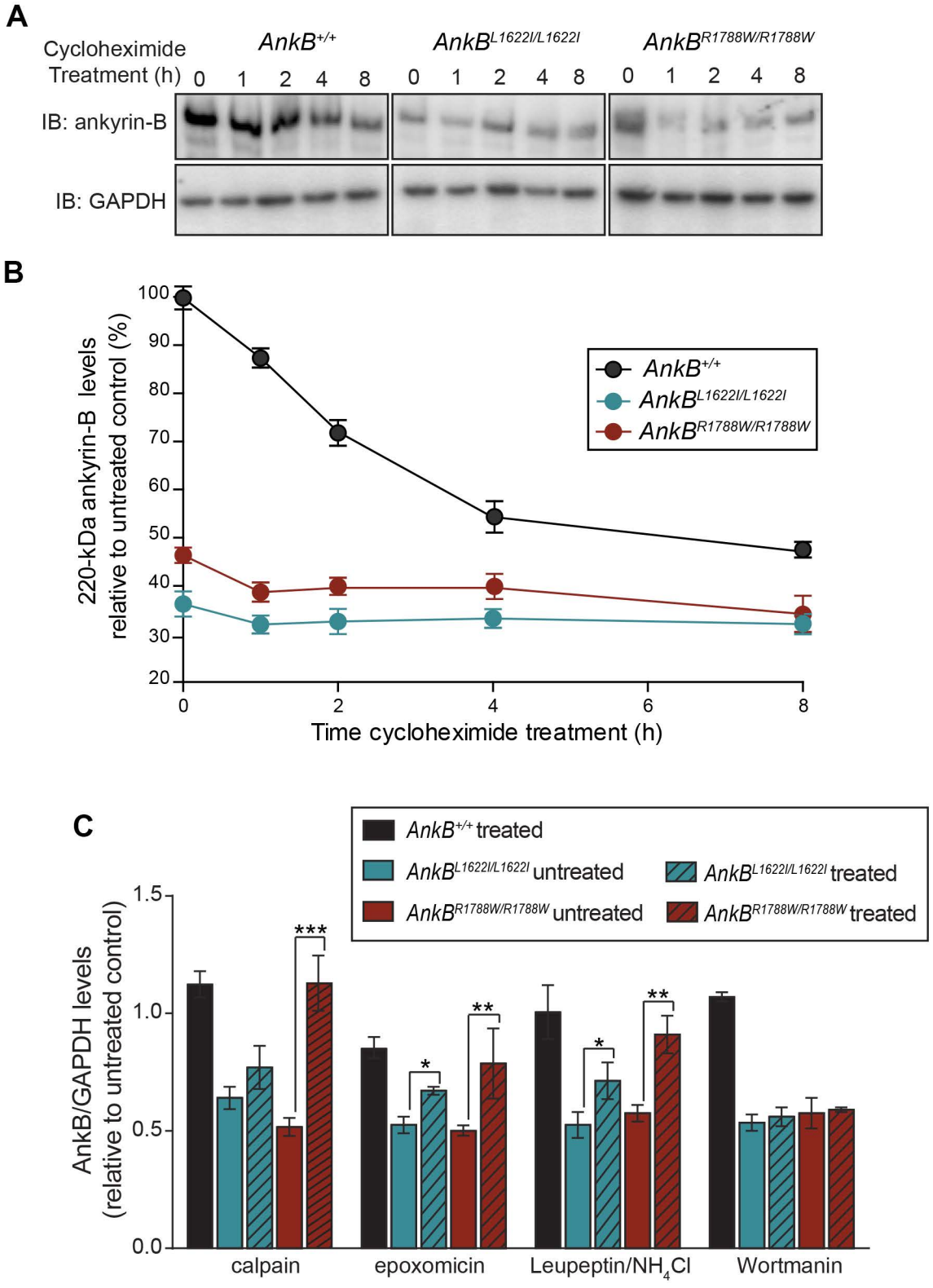

Figure S2. L1622I and R1788W variants cause loss of a less stable AnkB subpopulation. (A) Immunoblots of 220-kDa AnkB and GAPDH protein expression in MEFs treated with cycloheximide for the indicated time points. (B) Quantification of AnkB/GAPDH expression ratio as a percentage of levels in untreated control MEF cells. (C). Levels of AnkB proteins in primary MEF cultures in the absence or after treatment with inhibitors of various protein clearance pathways. Protein expression is given as AnkB/GAPDH levels relative to the same ratio in untreated control MEF cells. Data represent mean ± SEM (n=3 independent experiments). *p<0.05, **p<0.01 and ***p<0.001, one-way ANOVA with Tukey post-test.

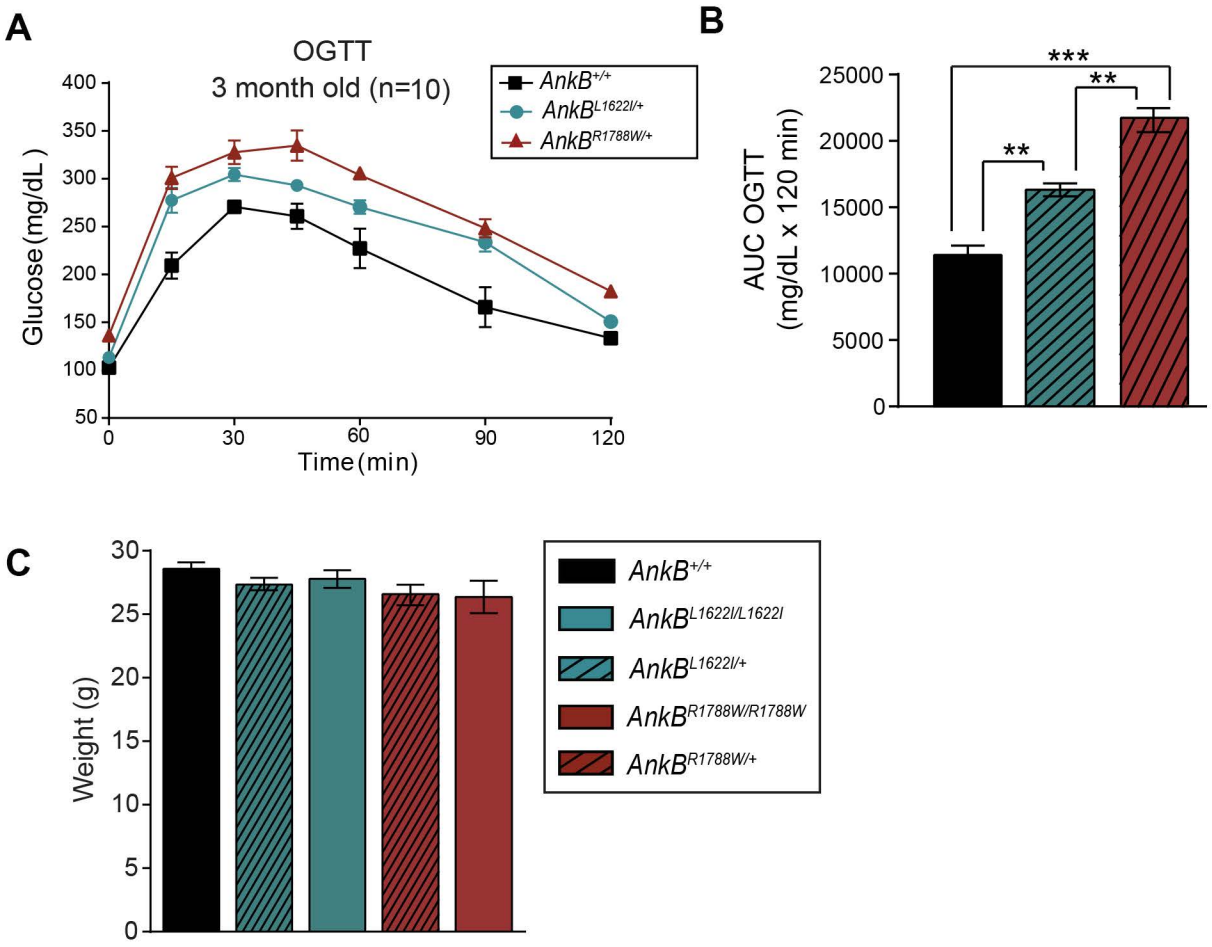

Figure S3. Oral glucose intolerance in young *AnkB*$^{R1788W/+}$ and *AnkB*$^{L1622I/+}$ mice. (A) Blood glucose levels in response to oral glucose (2 mg/kg body weight) corresponding to 3-month old *AnkB*$^{+/+}$, *AnkB*$^{R1788W/+}$, and *AnkB*$^{L1622I/+}$ mice. (B) Area under the curve (AUC) for oral glucose tolerance test (OGTT). (D) Total body weight at 3 months for mice of indicated genotypes. Data show mean ± SEM (n=10 mice per group) and is representative of three independent experiments. *p<0.05, **p<0.01 and ***p<0.001, one-way ANOVA with Tukey post-test.

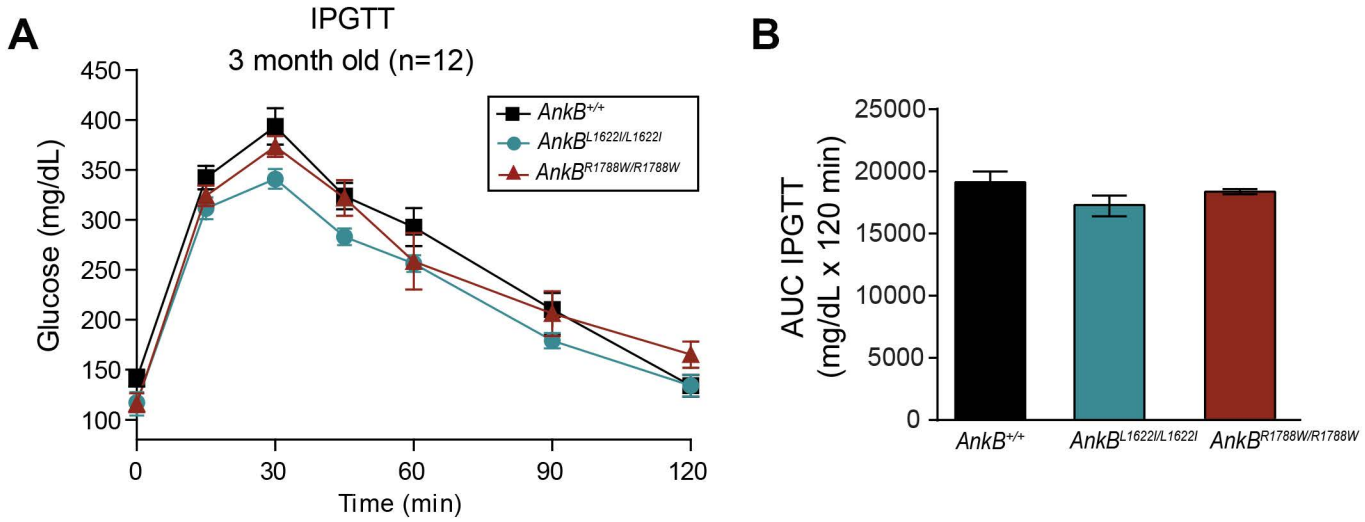

Figure S4. Normal intraperitoneal glucose tolerance in young *AnkB*$^{L1622I/L1622I}$ and *AnkB*$^{R1788W/R1788W}$ mice. (A) Blood glucose levels in response to intraperitoneal glucose (2 mg/kg body weight) administration. (B) Area under the curve (AUC) for intraperitoneal glucose tolerance test (IPTT). Data show mean ± SEM (n=12 mice per group) and is representative of three independent experiments. *p<0.05, one-way ANOVA with Tukey post-test.

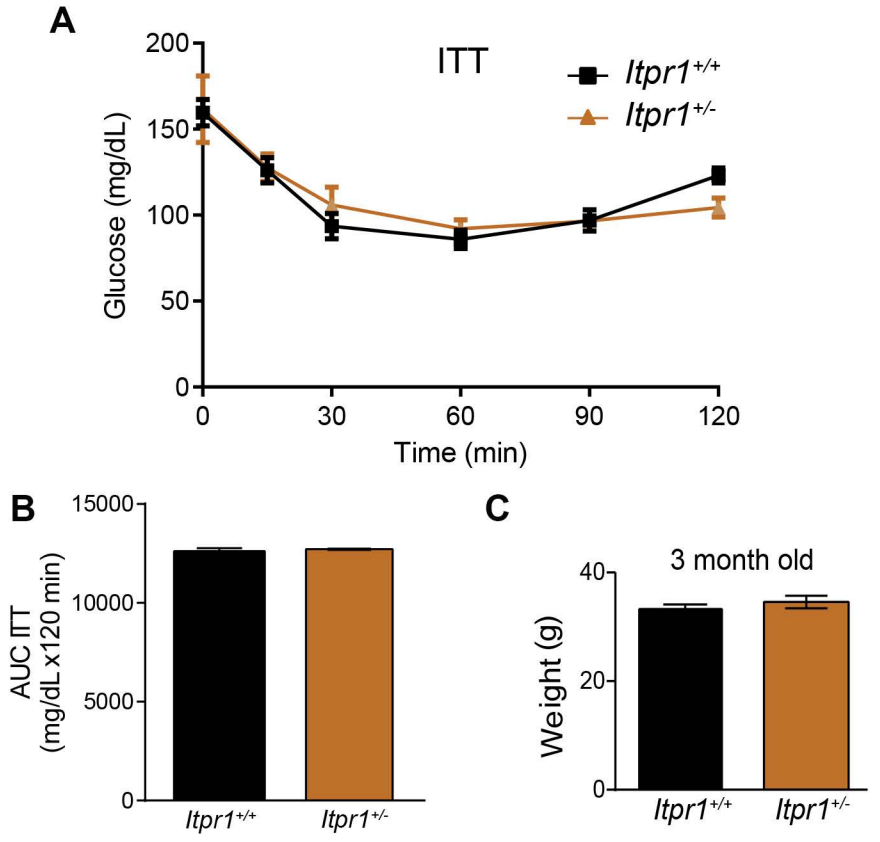

Figure S5. Young InsP3R haploinsufficient mice display normal insulin sensitivity. (A) Blood glucose levels in response to insulin administration (0.75U/kg) during an insulin tolerance test (ITT) for 3-month old control (*Itpr1*$^{+/+}$) and haploinsufficient InsP3R (*Itpr1*$^{+/-}$) mice. (B) Area under the curve (AUC) for an ITT. Data show mean ± SEM. (n=10 mice per group) and is representative of three independent experiments. *p<0.05, **p<0.01 and ***p<0.001, two-tailed t-test.

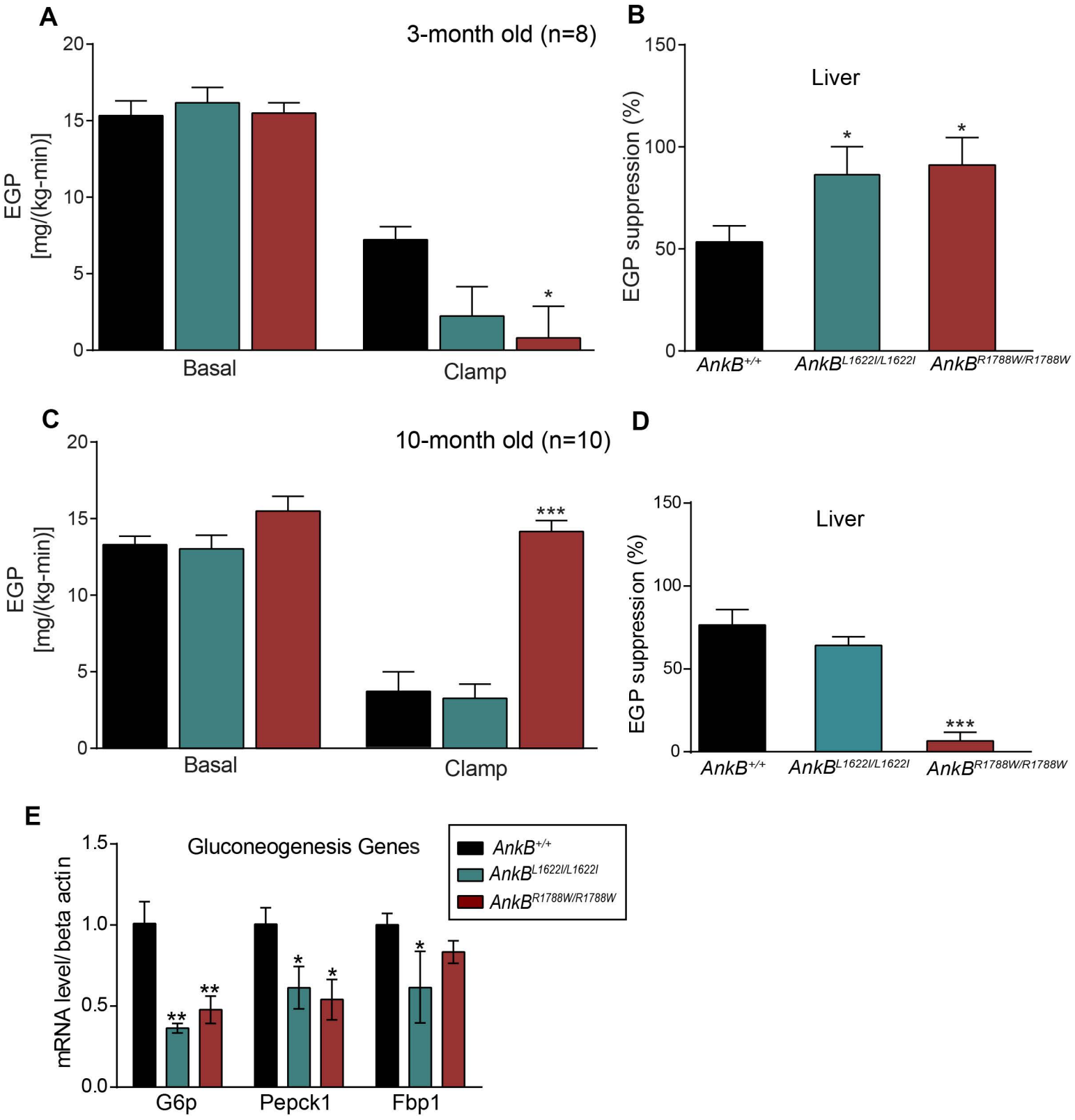

Figure S6. AnkB variants cause age-dependent changes in hepatic insulin sensitivity.
(A) Basal and insulin-stimulated (clamp) hepatic endogenous glucose production (EGP) rates determined during hyperinsulinemic euglycemic clamps for 3-month old (n=8) (A) and 10-month old (n=10) (C) mice. (B, D) Percentage of EGP suppression during clamp analysis for 3-month old (n=8) (B) and 10-month old (n=10) (D) mice. (E) Quantification of glucose-6-phosphatase (G6p), phosphoenolpyruvate carboxykinase 1 (Pepck1), and fructose 1, 6-bis phosphatase (Fbp1) transcript levels in liver of 3-month old mice. Levels of beta-actin transcript were used for normalization. Graph shown in E is representative of three independent determinations in three animals per each genotype. Data represent mean ± SEM. *p<0.05, **p<0.01 and ***p<0.001, one-way ANOVA with Tukey post-test).

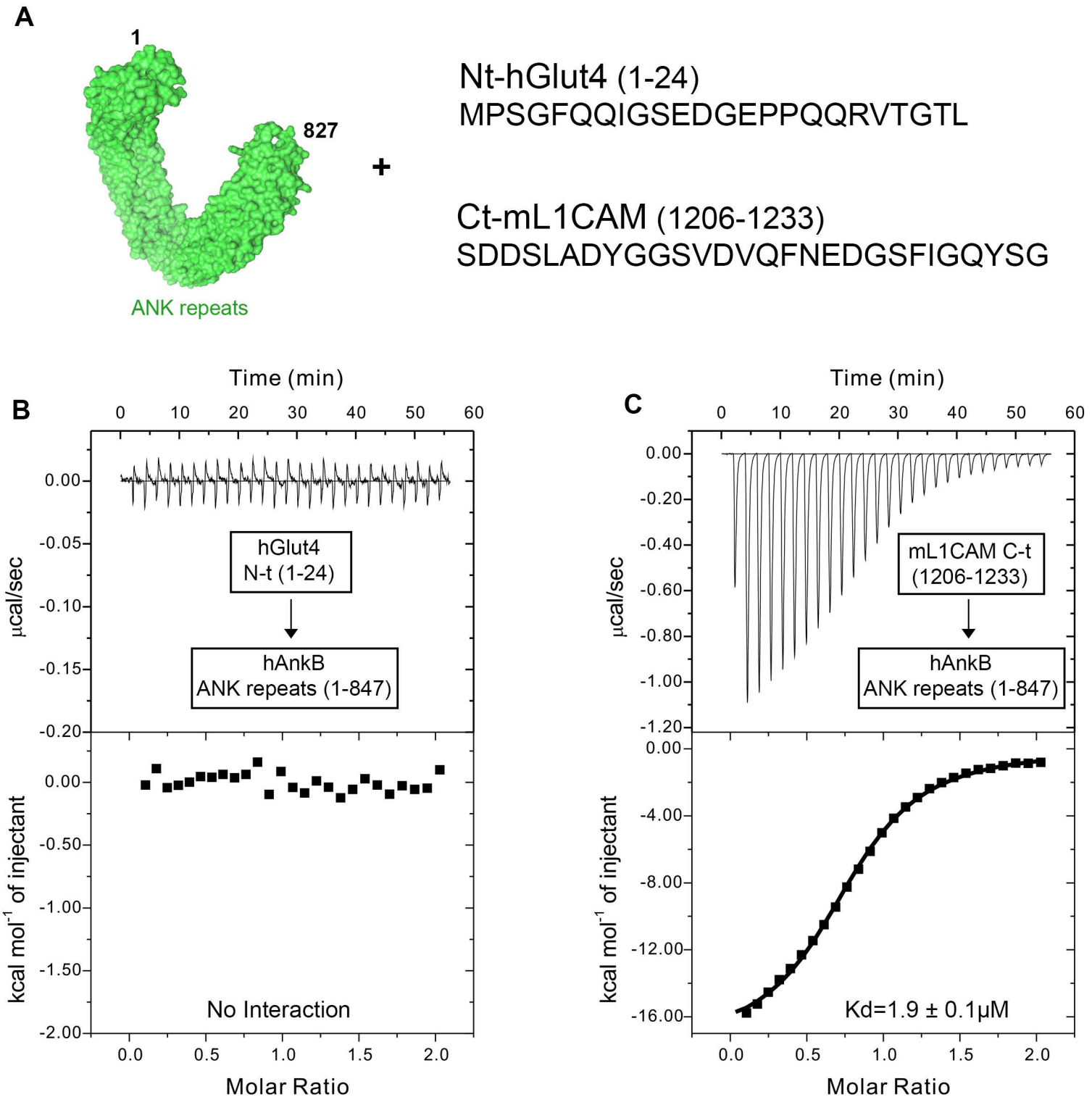

Figure S7. Characterization of the interaction between ANK repeats of AnkB and the N-terminal portion of GLUT4. (A) Schematic diagram of the ANK repeat domain of AnkB and the amino acid sequence corresponding to either residues 1-24 of human GLUT4 or 1206-1233 of the known ankyrin-binding domain (ABD) of mouse L1CAM. (B) ITC titration of a peptide of hGLUT4 (1–24) to AnkB repeats (1-847) shows no direct interaction. (C) ITC titration of the ABD of mL1CAM (1206-1233) to AnkB repeats (1-847) is shown as a positive control.

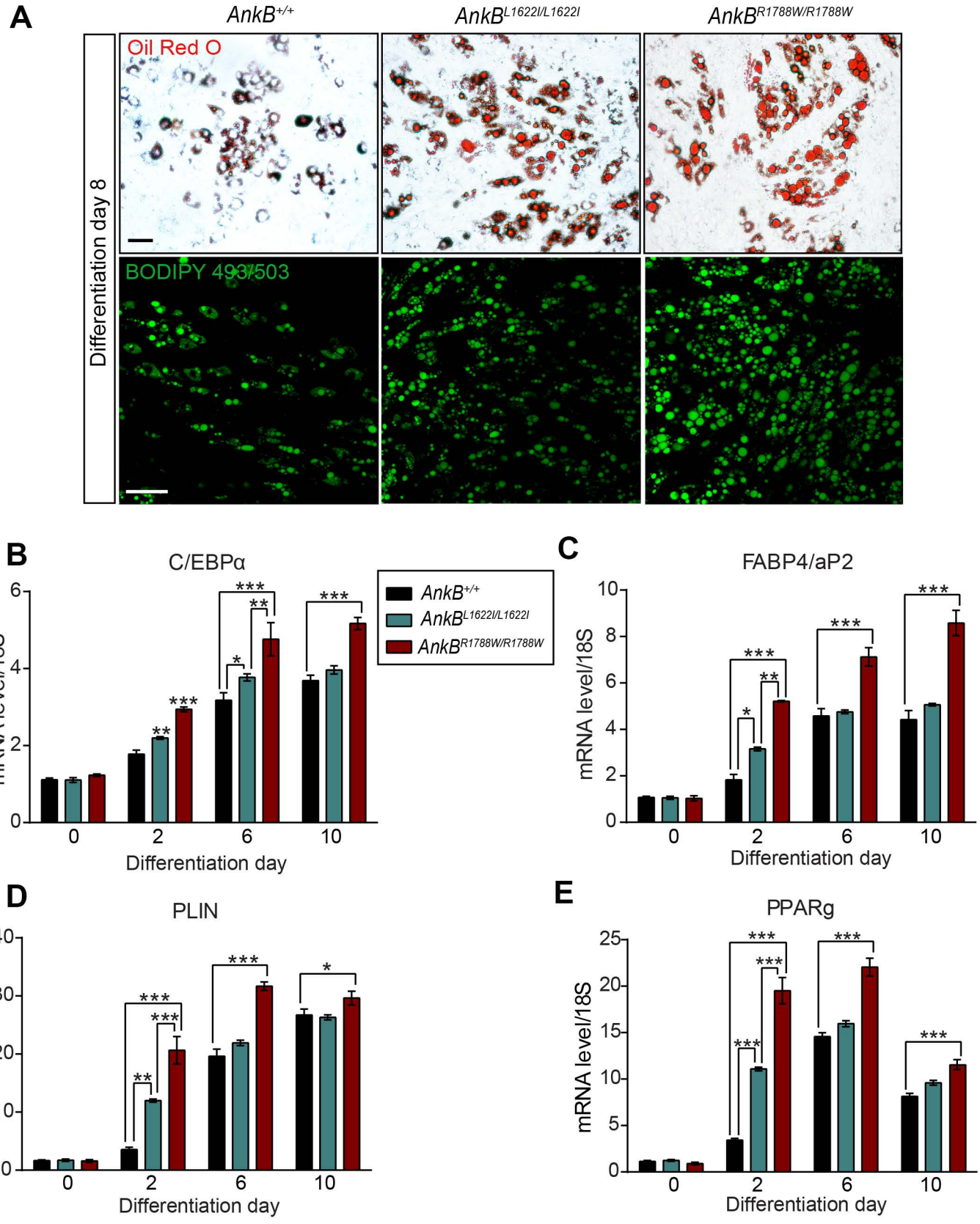

Figure S8. MEF from *AnkB*$^{R1788W/R1788W}$ and *AnkB*$^{L1622I/L1622I}$ mice differentiate into more and bigger adipocytes. (A) Oil red O (top) and BODIPY 493/507 (bottom) staining of day 8 differentiated adipocytes. Images are representative of 5 independent experiments. Scale bar, 10 μm. (B-E). Quantification of (B) CCAAT/enhancer binding protein alpha (C/ebpα), (C) fatty acid binding protein 4/ adipocyte protein 2 (Fabp4/aP2), (D) perilipin (Plin), and (E) peroxisome proliferator-activated receptor gamma (Pparg) transcript levels in differentiated adipocytes at different days post-differentiation. Levels of the 18S ribosomal subunit transcript were used for normalization. Data represent mean ± SEM from 12 independent preparations. *p<0.05, **p<0.01 and ***p<0.001, one-way ANOVA with Tukey post-test.

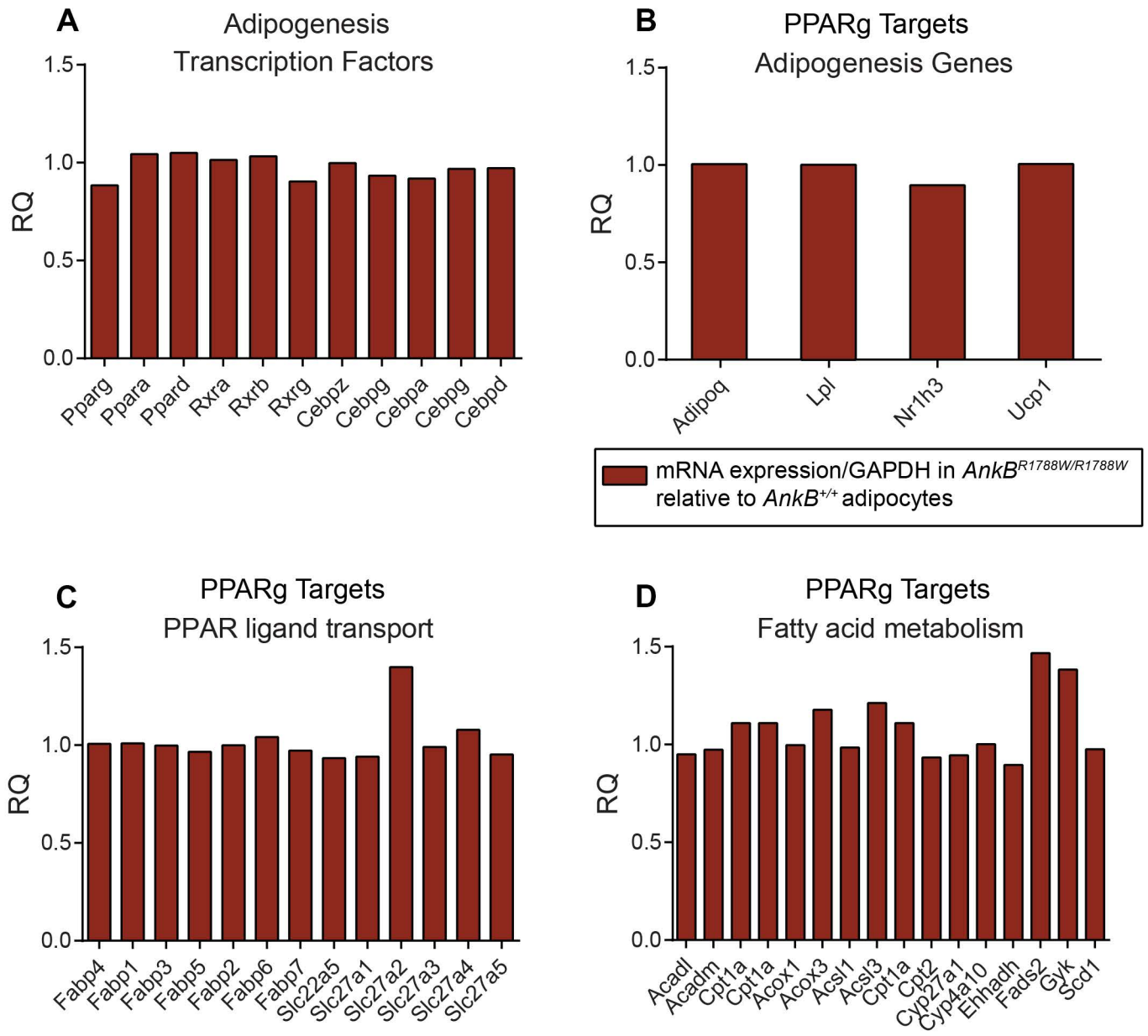

Figure S9. Young *AnkB*$^{R1788W/R1788W}$ mice show normal expression of adipogenesis-promoting genes before the onset of adiposity. (A). Relative expression of adipogenesis transcription factors transcripts in adipose tissue of 3-month old congenic male *AnkB*$^{R1788W/R1788W}$ mice. (B-D) Relative expression of transcript levels for PPARg target genes in adipose tissue of *AnkB*$^{R1788W/R1788W}$ mice. Levels of the GAPDH transcript were used for normalization. All data is reported as relative quantity (RQ) of target mRNA/GAPDH mRNA in *AnkB*$^{R1788W/R1788W}$ adipocytes relative to the same ratio in *AnkB*$^{+/+}$ cells. Data represent the mean of three mice per genotype for one experiment. Multi-way ANOVA analysis were performed to select target genes that were differentially expressed. *$p<0.05$.

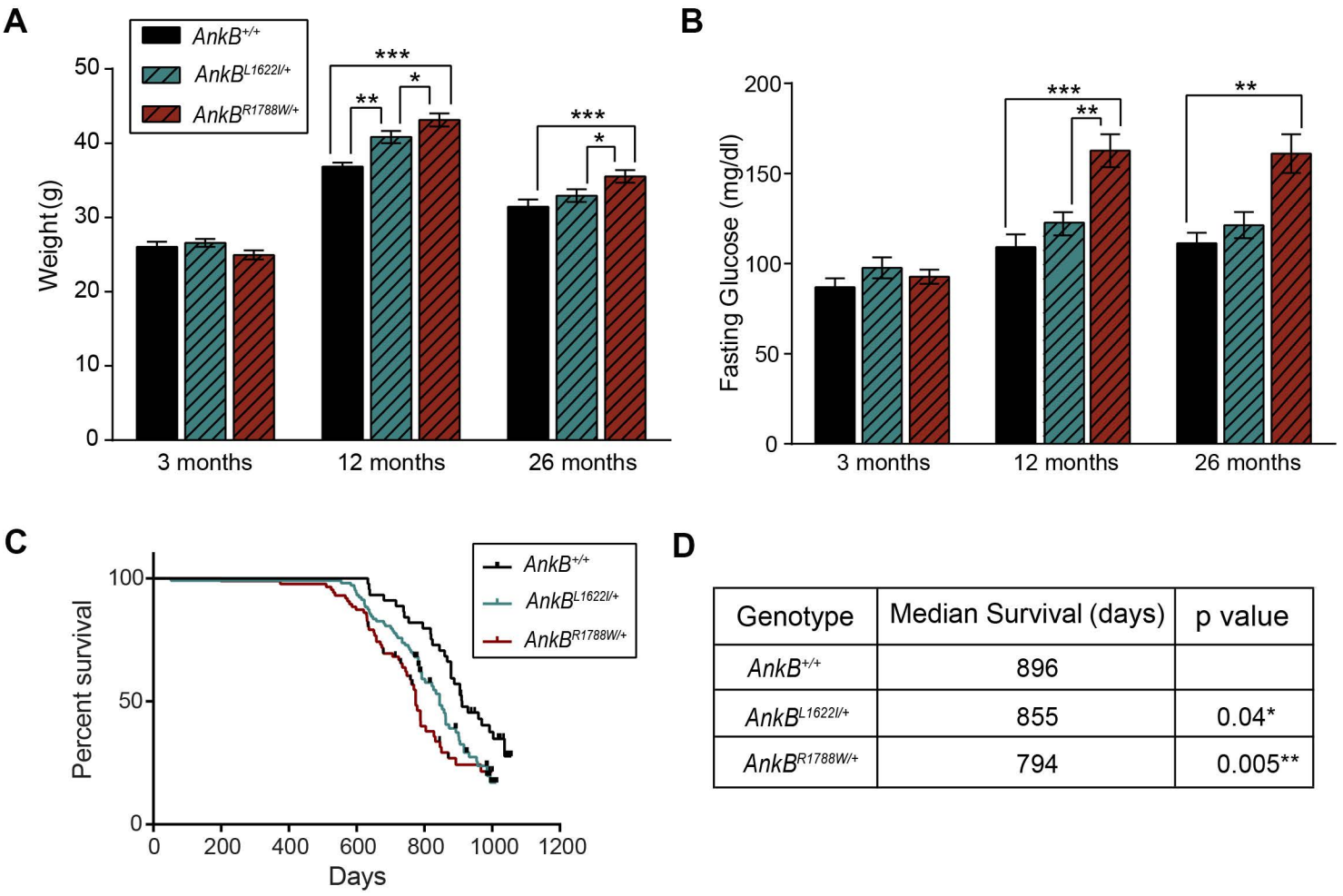

Genotype	Median Survival (days)	p value
AnkB$^{+/+}$	896	
AnkB$^{L1622I/+}$	855	0.04*
AnkB$^{R1788W/+}$	794	0.005**

Figure S10. Reduced life-span and age-dependent changes in body weight and fasting glucose in *AnkB*$^{R1788W/+}$ and *AnkB*$^{L1622I/+}$ mice. (A) Fasting glucose levels. (B) Body weights at indicated time points. Data represent mean ± SEM (n=50 mice per group, *p<0.05, **p<0.01 and ***p<0.001, one-way ANOVA with Tukey post-test). (C) Percent of survival during a 34 month long longevity study. (D) Reduced longevity of *AnkB*$^{R1788W/+}$ compared with *AnkB*$^{+/+}$ littermates and *AnkB*$^{L1622I/+}$ mice. Data for C and D were obtained from a total of n=100 mice per group, *p<0.05, **p<0.01, Mantel-Cox test.